IEEE Photonics Journal
An IEEE Photonics Society Publication

Open Access

Spectral-Efficient Reconstructed LACO-OFDM Transmission for Dimming Compatible Visible Light Communications

Volume 11, Number 1, February 2019

Baolong Li, *Member, IEEE*
Wei Xu, *Senior Member, IEEE*
Simeng Feng
Zhengquan Li, *Member, IEEE*

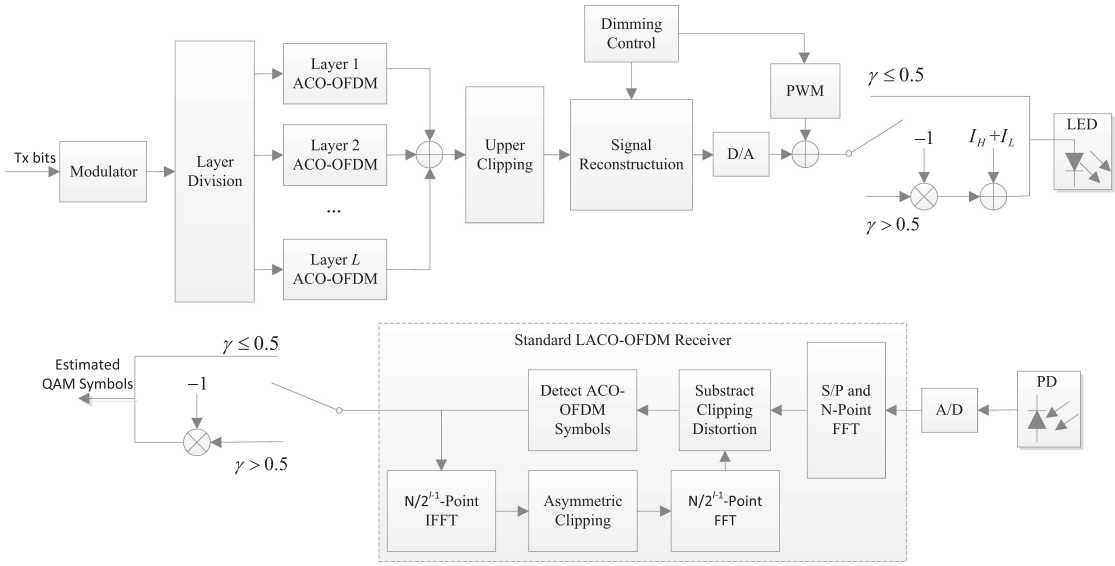

DOI: 10.1109/JPHOT.2019.2892849
1943-0655 © 2019 IEEE

Spectral-Efficient Reconstructed LACO-OFDM Transmission for Dimming Compatible Visible Light Communications

Baolong Li,[1,2] ***Member, IEEE***, **Wei Xu**,[2] ***Senior Member, IEEE***, **Simeng Feng**,[3] **and Zhengquan Li**,[1,4] ***Member, IEEE***

[1]Jiangsu Provincial Engineerinig Laboratory of Pattern Recognition and Computational Intelligence, Jiangnan University, Wuxi 214122, China
[2]National Mobile Communication Research Laboratory, Southeast University, Nanjing 210096, China
[3]Next Generation Wireless, School of Electronics and Computer Science, University of Southampton SO17 1BJ, UK.
[4]State key Laboratory of Networking and Switching Technology, Beijing University of Posts and Telecommunications, Beijing 100876, China

DOI:10.1109/JPHOT.2019.2892849

Manuscript received December 21, 2018; revised January 3, 2019; accepted January 9, 2019. Date of publication January 14, 2019; date of current version January 31, 2019. This work was supported in part by the National Natural Science Foundation of China unders Grant 61871109, 61571108, 61701197, and 61801193; in part by the Six talent peaks project in Jiangsu Province under Grant GDZB-005; in part by the Royal Academy of Engineering under the Distinguished Visiting Fellowship scheme; in part by the open research fund of National Mobile Communications Research Laboratory, Southeast University (No. 2019D18). Corresponding authors: Wei Xu, Zhengquan Li (e-mail: wxu@seu.edu.cn, lzq722@jiangnan.edu.cn).

Abstract: Dimming control is critical in practical visible light communication (VLC) systems to satisfy illumination demand. Upon exploiting multiple layers of asymmetrically clipped optical orthogonal frequency division multiplexing (ACO-OFDM) signals for simultaneous transmission, layered ACO-OFDM (LACO-OFDM) constitutes a promising spectral-efficient modulation technique for VLC. However, dimming by integrating the industry-preferred pulsewidth modulation (PWM) to the LACO-OFDM scheme induces severe clipping noise due to the nonlinearity of LEDs. In this paper, we conceive a reconstructed LACO-OFDM (RLACO-OFDM) scheme incorporating the PWM technique for VLC to accommodate the dimming demands for indoor illumination, while maintaining a spectral-efficient communication link. Moreover, superior to its counterparts, the transmitted symbols in the RLACO-OFDM based VLC system can be readily recovered by a standard LACO-OFDM receiver while no additional detection of the PWM signal is required, which reduces the receiver complexity. Numerical results demonstrate that the proposed RLACO-OFDM is capable of realizing high spectral efficiency over a broad dimming range.

Index Terms: Visible light communication (VLC), dimming control, pulse width modulation (PWM), asymmetrically clipped optical orthogonal frequency division multiplexing (ACO-OFDM), layered ACO-OFDM.

1. Introduction

As a benefit of its distinctive advantages, such as license-free operations, inherent high security, low-cost implementation, etc, visible light communication (VLC) has attracted significant attention

[1], [2]. Given the urgent customer demand for high-speed data transmission and the saturation of the radio frequency (RF) spectrum resource, VLC is deemed as a promising technology to realize ubiquitous wireless coverage typically for indoor environment [3]–[5].

Due to the robustness to inter-symbol interference (ISI) and high spectral efficiency, orthogonal frequency division multiplexing (OFDM) has been extensively investigated in VLC to achieve gigabit transmission [6]–[8]. In VLC, the transmitted signal is constrained to be nonnegative as a result of inherent nature of LEDs [9]. Therefore, many specific solutions have been proposed to generate nonnegative time-domain optical OFDM (O-OFDM) signals. One of the popular solutions is known as direct-current-offset optical OFDM (DCO-OFDM), which produces nonnegative signals by directly adding a direct current (DC) component [10]. However, the DC component does not convey any information, leading to power inefficiency [11]. Some power-efficient strategies have been proposed, including asymmetrically clipped optical OFDM (ACO-OFDM) [12] and pulse-amplitude-modulated discrete multitone (PAM-DMT) [13]. Since only half of the subcarriers or signal dimensions are actively utilized in both ACO-OFDM and PAM-DMT, a hybrid ACO-OFDM (HACO-OFDM) scheme in [14] has amalgamated the techniques of ACO-OFDM and PAM-DMT to enhance spectral efficiency. However, HACO-OFDM still does not fully exploit the frequency-domain resource since the real part of even subcarriers is unmodulated. Recently, a layered ACO-OFDM (LACO-OFDM) has been developed to further improve the spectral efficiency, where multiple layers of ACO-OFDM are superimposed in the time domain for simultaneous transmission [15].

In VLC, dimming control is a critical issue since integrating efficient dimming techniques into VLC can significantly improve energy savings, as well as achieve the brightness adjustment of LEDs according to personal preferences [16]. In the context of OFDM-based VLC, there are mainly two kinds of dimming techniques for illumination control, namely, analog and digital approaches [17]. In the analog approach, the biasing and scaling of the O-OFDM signal are jointly adjusted to achieve efficient illumination control. Appealing works about the analog approaches include asymmetrical hybrid optical OFDM (AHO-OFDM) [18], enhanced DCO-OFDM (eDCO-OFDM) [19], and dimmable O-OFDM (DO-OFDM) [20]. It has been shown that these schemes can support a high link capacity for a wide dimming range. However, the challenge of implementing the analog approaches stems from the fact that the coefficients of the VLC system, such as scaling factors and biasing, highly depend on the dimming requirement, which can make the detection process of the O-OFDM signals sensitive to the dimming level [21].

Alternatively, various digital dimming techniques have been conceived for OFDM-based VLC. To elaborate, the scheme proposed in [22] transmitted O-OFDM signal during the ON state of the pulse width modulation (PWM) signal to achieve the functionalities of both dimming and communication, which is easy to implement but causes the reduction of data rate due to the waste of the OFF state. In [23], the time-domain O-OFDM signal was multiplied by a periodic PWM signal for simultaneous transmission. However, this scheme can not support high-speed VLC systems since the bandwidth of the PWM is required to be at least twice of the O-OFDM signal. In order to combine the wideband O-OFDM signal with relatively narrowband PWM signal, reverse polarity optical-OFDM (RPO-OFDM) has been proposed in [24], in which the polarity of the ACO-OFDM symbols is reversed during the ON state. Nevertheless, in order to re-adjust the reverse polarity, additional detection operation of the PWM signal is required before decoding the ACO-OFDM signal. The detection of the PWM signal may become intricate especially in multiple-LED scenarios [25], [26], since multi-path PWM signals from different LEDs are coupled at the receiver and difficult to de-multiplex. Furthermore, a negative HACO-OFDM (NHACO-OFDM) has been introduced in [21] and then combined with the original HACO-OFDM scheme for dimming control, which exhibits a high power and spectrum efficiency for a broad dimming range. Recently, the idea has been further extended in [27] to the LACO-OFDM and a spectral-efficient dimmable VLC system has been realized by incorporating the negative LACO-OFDM (NLACO-OFDM) with the original LACO-OFDM. In both schemes, the subtraction of the clipping noise at the receiver depends on whether the original or the negative signal is transmitted, since the clipping procedure of the original O-OFDM is different from the negative O-OFDM. Therefore, similar to RPO-OFDM, additional detection operation of the transmitted O-OFDM is required at the receiver.

Against this background, a novel dimmable reconstructed LACO-OFDM (RLACO-OFDM) scheme relying on the PWM technique is conceived for providing spectral-efficient VLC, while concurrently satisfying various dimming requirements. A direct superimposition of the conventional LACO-OFDM and PWM signals yields severe clipping distortion. In the proposed scheme, we introduce a reconstruction procedure of the LACO-OFDM signal to restrict the superimposed signal operate within the linear dynamic range, so that the dynamic range of LEDs can be fully exploited. Moreover, superior to its counterparts, the decoding process of the proposed RLACO-OFDM can be directly accomplished by a standard LACO-OFDM receiver while no additional detection operation of PWM is required. It leads to relatively low complexity and makes our proposed scheme more suitable for practical implementation especially in multiple-LED scenarios. Numerical results demonstrate that the proposed RLACO-OFDM is capable of supporting a high spectral efficiency over a broad dimming range.

2. Layered ACO-OFDM

LACO-OFDM exploits the property of the Fourier transform and combines the multiple layers of ACO-OFDM signals for simultaneous transmission. It achieves higher power and spectral efficiency than the conventional O-OFDM schemes. In the l-th layer of LACO-OFDM, only the $2^{l-1}(2m+1)$-th ($m = 0, 1, \ldots, N/2^l - 1$) subcarriers are modulated while the remaining subcarriers are set to zeros [27]. After inverse fast Fourier transform (IFFT) operation, the generated time-domain signal of the l-th layer is expressed as [15]

$$\begin{aligned} x_{\mathrm{A},n}^{(l)} &= \frac{1}{\sqrt{N}} \sum_{i=0}^{N-1} X_{\mathrm{A},i}^{(l)} \exp\left(\frac{j2\pi ni}{N}\right) \\ &= \frac{1}{\sqrt{N}} \sum_{m=0}^{N/2^l-1} X_{\mathrm{A},2^{l-1}(2m+1)}^{(l)} \exp\left(\frac{j2\pi}{\frac{N}{2^{l-1}}} n(2m+1)\right), \end{aligned} \tag{1}$$

where $j = \sqrt{-1}$, $X_{\mathrm{A},i}^{(l)}$ denotes the frequency-domain signal of the l-th layer. From (1), it follows that $x_{\mathrm{A},n}^{(l)} = x_{\mathrm{A},n+N/2^{l-1}}^{(l)}$, which implies that $x_{\mathrm{A},n}^{(l)}$ is a periodic function with period of $\frac{N}{2^{l-1}}$. Furthermore, define the $N/2^{l-1}$-length frequency-domain signal as

$$X_i^{(l)} = \begin{cases} 0, & i = 2m, \\ X_{\mathrm{A},2^{l-1}(2m+1)}^{(l)}, & i = 2m+1, \end{cases} \tag{2}$$

which is the typical signal structure of ACO-OFDM in frequency domain. Performing $N/2^{l-1}$-point IFFT of $X_i^{(l)}$ yields the unclipped time-domain signal of ACO-OFDM, denoted by $x_n^{(l)}$. In practice, the time-domain signal $x_{\mathrm{A},n}^{(l)}$ of the l-th layer can be obtained by repeating the $N/2^{l-1}$-length signal $x_n^{(l)}$ by 2^{l-1} times [27]. Additionally, since only the odd subcarriers of $X_i^{(l)}$ are modulated while the even subcarriers remain unoccupied, $x_n^{(l)}$ follows the anti-symmetry that $x_n^{(l)} = -x_{n+N/2^l}^{(l)}$, which means the negative parts can be directly clipped at zero without any information loss.

In LACO-OFDM, time-domain signal is generated through the superimposition of multiple layers of the ACO-OFDM signals, which is expressed as [15]

$$x_{\mathrm{LACO},n} = \sum_{l=1}^{L} \left\lfloor x_{\mathrm{A},n}^{(l)} \right\rfloor_c, \; n = 0, 1, \ldots, N-1, \tag{3}$$

where $x_{\mathrm{LACO},n}$ denotes the time-domain signal of LACO-OFDM, L is the total number of the layers, and $\lfloor x \rfloor_c = \max\{x, 0\}$ denotes the clipping operation of negative parts. In general, the variance of modulated symbols is set to be uniform as σ^2 for all the L layers of ACO-OFDM. Since $N/2^l$ subcarriers are modulated in Layer l, the variance of the unclipped signal $x_{\mathrm{A},n}^{(l)}$ is $\sigma^2/2^l$ [20].

The clipping distortion of the l-th layer In LACO-OFDM falls on the $m2^l$-th ($m = 0, 1, \ldots, N/2^l - 1$) subcarriers of the LACO-OFDM signals, where the $(l+1)$th layer is modulated, and it does not

interfere with the transmitted symbols of lower layers [15]. Therefore, the transmitted symbols in the first layer are ideally free of interference and can be readily recovered at the receiver by directly performing the FFT operation. Then, the interference caused by the first layer is regenerated based on the estimated symbols. After subtracting the regenerated interference from the received signals, the transmitted symbols of the second layer can be subsequently estimated. Similarly, the transmitted symbols in the remaining higher layers are detected successively at the receiver through the interference cancellation.

3. Dimmable VLC System Based on Reconstructed LACO-OFDM

Dimming control is an essential requirement for VLC. In this section, we propose a PWM-based RLACO-OFDM with dimming control to provide a spectral-efficient VLC transmission, while accommodating dimming demands for illumination.

3.1 Pulse Width Modulation

PWM is an industry-preferred solution to achieve the illumination control of LEDs over a wide dimming range. In PWM, a periodic train of pulses is transmitted, and the width of the pulse can be adjustable to provide the required dimming level. Given the limited dynamic range of LEDs, the PWM signal is expressed as

$$x_{\mathrm{PWM}}(t) = \begin{cases} I_H, & 0 \le t \le T, \\ I_L, & T < t \le T_{\mathrm{PWM}}, \end{cases} \tag{4}$$

where I_H and I_L respectively denote the maximum and minimum current levels permitted by the LEDs, T_{PWM} denotes the time period of the PWM signal, and T is the width of the pulse. Regions $[0, T]$ and $(T, T_{\mathrm{PWM}}]$ denote the ON and OFF states of the PWM signal, respectively. The duty cycle of the PWM signal is defined as $\rho \triangleq T/T_{\mathrm{PWM}}$.

In the proposed scheme, the period of PWM is set to $T_{\mathrm{PWM}} = N_s T_s$, where N_s denotes the number of LACO-OFDM symbols during one PWM period and T_s is the LACO-OFDM symbol period. Furthermore, the width of the pulse of the PWM signal can be adjusted in the unit of T_s, i.e., $T = N_d T_s$, where N_d represents the number of LACO-OFDM symbols occupying the ON duration of the PWM signal. Then, the duty cycle of the PWM signal is calculated as $\rho = N_d/N_s$.

3.2 Reconstructed LACO-OFDM

In order to support dimming functionality as well as a reliable broadband communication link, the PWM dimming technique is required to be integrated into LACO-OFDM. However, a direct superimposition of LACO-OFDM and PWM signals can result in the LED operating in the nonlinear region, which causes severe clipping distortion, as seen in Fig. 1. To address this issue, we propose a novel RLACO-OFDM scheme by introducing a signal reconstruction procedure of LACO-OFDM, which makes the superimposed signal be restricted within the linear dynamic range.

In the OFF duration of the PWM, the LACO-OFDM signal $x_{\mathrm{LACO},n}$ can be directly transmitted through PWM due to the non-negativity of LACO-OFDM. However, a negative signal is required to be superimposed on the ON state of the PWM as a result of the limited dynamic range of LEDs. Observing the sequence $\{x_{\mathrm{LACO},n+kN/2^L},\ k = 0, 1, \ldots, 2^L - 1\}$, we define a periodic signal s_n with period $N/2^L$, i.e., $s_n = s_{n+N/2^L}$. For $0 \le n \le N/2^L - 1$, s_n is given by

$$s_n = \max_{0 \le k \le 2^L - 1} \left\{ x_{\mathrm{LACO},n+kN/2^L} \right\}, \tag{5}$$

where the value of s_n is the maximum in the sequence $\{x_{\mathrm{LACO},n+kN/2^L},\ k = 0, 1, \ldots, 2^L - 1\}$. Then, a negative signal is generated by subtracting s_n from $x_{\mathrm{LACO},n}$, which can be directly transmitted onto the ON state of the PWM signal. Consequently, by introducing the periodic signal s_n, we define the

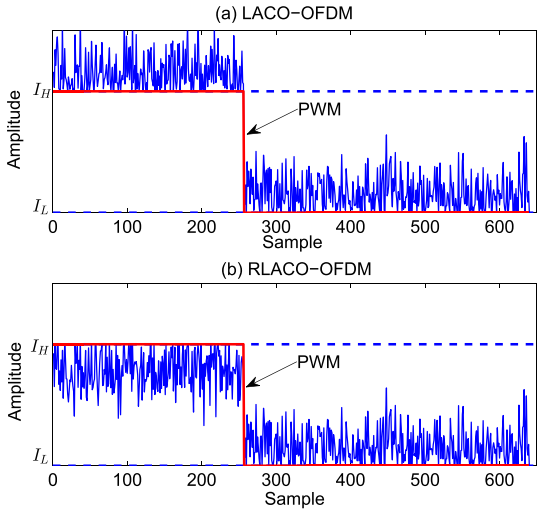

Fig. 1. A demonstration of the superimposed signal with 64-point FFT and $\rho = 0.4$. (a) Superimposition of the PWM and LACO-OFDM signals. (b) Superimposition of the PWM and RLACO-OFDM signals.

RLACO-OFDM signal as

$$x_{\text{RLACO},n} = \begin{cases} x_{\text{LACO},n}, & \text{OFF state,} \\ x_{\text{LACO},n} - s_n, & \text{ON state.} \end{cases} \tag{6}$$

Assume that $x_{\text{LACO},n}$ is pre-clipped to fit the dynamic range of the LEDs, i.e., $0 \le x_{\text{LACO},n} \le I_H - I_L$. Then, we have $0 \le s_n \le I_H - I_L$. Since s_n is the maximum value in the sequence $\{x_{\text{LACO},n+kN/2^L},\ k = 0, 1, \ldots, 2^L - 1\}$, it follows that $I_L - I_H \le x_{\text{LACO},n} - s_n \le 0$. Therefore, we have $I_L \le x_{\text{RLACO},n} + I_L \le I_H$ and $I_L \le x_{\text{RLACO},n} + I_H \le I_H$ during the OFF and ON states of PWM, respectively, which means that the superimposed signal of RLACO-OFDM and PWM is restricted within the dynamic range of LEDs, as shown in Fig. 1. Therefore, compared to the conventional LACO-OFDM, the nonlinear distortion can be effectively suppressed in the proposed RLACO-OFDM when combined with the PWM signal.

Now we prove that $x_{\text{RLACO},n}$ can be directly detected by the standard LACO-OFDM receiver architecture. In LACO-OFDM, successive interference cancellation is used at the receiver to detect the LACO-OFDM signals since the clipping of each layer induces the inter-layer interference imposed on the higher layers. Note that the RLACO-OFDM signal in (6) consists of two components, i.e., the original LACO-OFDM signal $x_{\text{LACO},n}$ and the introduced signal s_n. Next, we will show that the introduced signal s_n does not disturb the legitimate data symbols conveyed by all the L layers of the LACO-OFDM signal $x_{\text{LACO},n}$. In this case, the RLACO-OFDM signal can be directly detected by the standard LACO-OFDM receiver regardless of the interference caused by s_n. More specifically, after performing the N-point FFT of s_n, we have

$$\begin{aligned} S_i &= \frac{1}{\sqrt{N}} \sum_{n=0}^{N-1} s_n \exp\left(\frac{-j2\pi ni}{N}\right) \\ &= \frac{1}{\sqrt{N}} \sum_{n=0}^{N/2^L-1} \sum_{k=0}^{2^L-1} s_{n+\frac{kN}{2^L}} \exp\left(\frac{-j2\pi\left(n + kN/2^L\right)i}{N}\right) \\ &= \frac{1}{\sqrt{N}} \sum_{n=0}^{N/2^L-1} \left[s_n \exp\left(\frac{-j2\pi ni}{N}\right) \sum_{k=0}^{2^L-1} \exp\left(\frac{-j2\pi ki}{2^L}\right) \right] \\ i &= 0, 1, \ldots, N-1. \end{aligned} \tag{7}$$

The above equation accrues from the fact that s_n is a periodic signal with period $N/2^L$. Since

$$\sum_{k=0}^{2^L-1} \exp\left(\frac{-j2\pi ki}{2^L}\right) = \begin{cases} 2^L, & i = m2^L, \\ 0, & \text{otherwise}, \end{cases} \tag{8}$$

where $m = 0, 1, \ldots, N/2^L - 1$, we have

$$S_i = \begin{cases} \frac{2^L}{\sqrt{N}} \sum_{n=0}^{N/2^L-1} s_n \exp\left(\frac{-j2\pi ni}{N}\right), & i = m2^L, \\ 0, & \text{otherwise}. \end{cases} \tag{9}$$

It is observed that S_i only falls on the $m2^L$-th ($m = 0, 1, \ldots, N/2^L - 1$) subcarriers which are not used for data transmission in the LACO-OFDM with L layers, and they do not interfere with the transmitted data symbols in the first L layers. Therefore, without taking the influence of the introduced signal s_n into consideration, we can directly adopt the standard LACO-OFDM receiver to decode the transmitted symbols in the proposed reconstructed signal, $x_{\text{RLACO},n}$.

3.3 RLACO-OFDM Based Dimming Control

Upon introducing the RLACO-OFDM signal, the functionality of dimming control can be readily integrated into the broadband VLC system by directly combining the PWM and RLACO-OFDM signals. The superimposed signal for both dimming and communication is expressed as

$$y_n = x_{\text{RLACO},n} + s_{\text{PWM},n}, \tag{10}$$

where $s_{\text{PWM},n}$ denotes the nth sample of $s_{\text{PWM}}(t)$. Note that the PWM signal $s_{\text{PWM},n}$ is a constant of I_L or I_H sustained in one OFDM symbol, which only affects the signal component at the zero-th subcarrier at the receiver. Therefore, the dimming signal y_n can be directly decoded by the standard LACO-OFDM receiver, like $x_{\text{RLACO},n}$. For the superimposed signal y_n, adjusting the duty cycle of the PWM signal can change the dimming level which is defined as

$$\gamma = \frac{I_{\text{Avg}} - I_L}{I_H - I_L}. \tag{11}$$

Here, I_{Avg} is the average amplitude of the signal y_n. Assume that y_n achieves the dimming level of $\gamma \leq 0.5$. Based on the definition of the dimming level, the average amplitude of y_n is equal to $I_{\text{Avg}} = I_L + (I_H - I_L)\gamma$. Furthermore, considering the signal $I_H + I_L - y_n$, we can observe that the average amplitude of the signal is calculated as $I_{\text{Avg}} = I_H - (I_H - I_L)\gamma$, which indicates that a dimming level of $1 - \gamma$ is achieved. Therefore, in order to reach a relatively symmetric dimming results in the ranges of [0,0.5] and (0.5,1], the RLACO-OFDM based dimming signal is given by

$$y_{\text{dim},n} = \begin{cases} y_n, & \gamma \leq 0.5, \\ I_H + I_L - y_n, & \gamma > 0.5. \end{cases} \tag{12}$$

Similar to the case of $\gamma \leq 0.5$, the standard LACO-OFDM receiver can be adopted to detect the received signal for $\gamma > 0.5$, and then the polarity is re-justed to yield the originally transmitted symbols. Additionally, the information about whether the dimming level is greater than 0.5 can be readily obtained at the receiver, such as through sending it from the transmitter, which requires only a relatively low overhead of one bit. Finally, the schematic of the proposed dimmable RLACO-OFDM is depicted in Fig. 2.

4. Theoretical Dimming Performance Analysis

In this section, we theoretically analyze the dimming level achieved by the RLACO-OFDM scheme. From (11), the dimming level depends on the average amplitude of the signal. For $\gamma \leq 0.5$, the

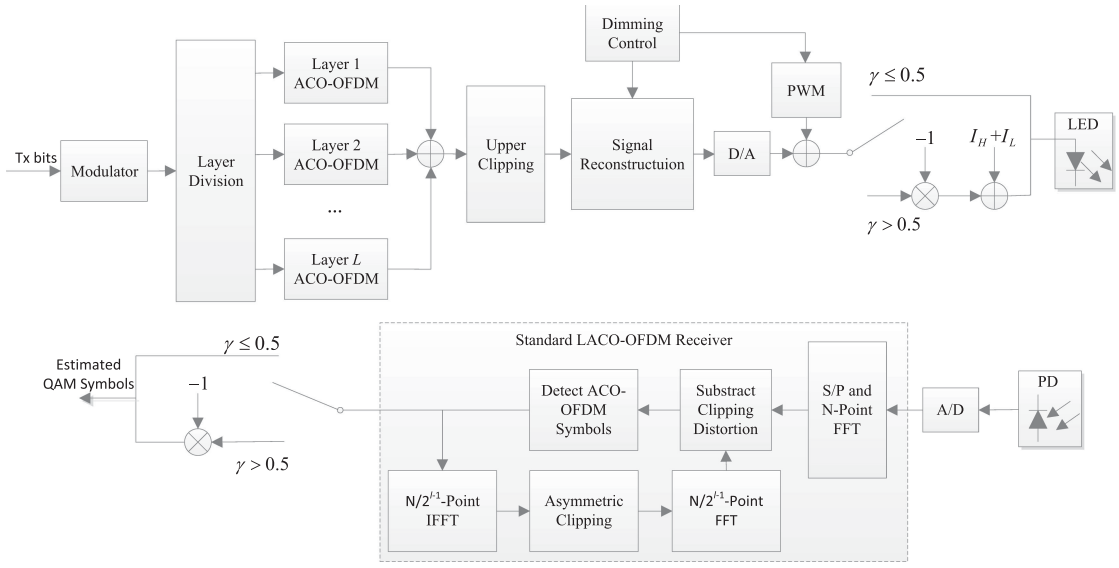

Fig. 2. Transmitter and receiver of the proposed dimmable RLACO-OFDM.

average amplitude is calculated as

$$\begin{aligned} I_{\text{avg}} &= \frac{\left(I_L + \mathrm{E}\left\{x_{\text{LACO},n}\right\}\right)\left(T_{\text{PWM}} - T\right)}{T_{\text{PWM}}} + \frac{\left(I_H + \mathrm{E}\left\{x_{\text{LACO},n}\right\} - \mathrm{E}\left\{s_n\right\}\right)T}{T_{\text{PWM}}} \\ &= \left(I_L + a_1\right)\left(1-\rho\right) + \left(I_H + a_1 - a_2\right)\rho \\ &= \left(I_H - I_L - a_2\right)\rho + I_L + a_1, \end{aligned} \tag{13}$$

where $\mathrm{E}\{\cdot\}$ denotes the statistical expectation, and $a_1 \triangleq \mathrm{E}\left\{x_{\text{LACO},n}\right\}$ and $a_2 \triangleq \mathrm{E}\left\{s_n\right\}$ are the expectations of $x_{\text{LACO},n}$ and s_n, respectively. Note that a_1 and a_2 could be readily obtained through numerical methods given the generated signals. Nevertheless, a specific method is presented to theoretically calculate the expectation of the signal. Given the limited linear dynamic range of LEDs, a_1 and a_2 are expressed as

$$\begin{aligned} a_1 &= \int_0^{I_H - I_L} x f_{x_{\text{LACO},n}}(x)dx + \int_{I_H - I_L}^{+\infty} (I_H - I_L) f_{x_{\text{LACO},n}}(x)dx, \\ a_2 &= \int_0^{I_H - I_L} s f_{s_n}(s)ds + \int_{I_H - I_L}^{+\infty} (I_H - I_L) f_{s_n}(s)ds, \end{aligned} \tag{14}$$

where $f_{x_{\text{LACO},n}}(x)$ and $f_{s_n}(s)$ are the probability density functions (PDF) of $x_{\text{LACO},n}$ and s_n, respectively. It is clearly observed that the computation of a_1 and a_2 mainly relies on $f_{x_{\text{LACO},n}}(x)$ and $f_{s_n}(s)$. Note that the PDF $f_{x_{\text{LACO},n}}(x)$ has been investigated in [28]. Therefore, we focus on the calculation of $f_{s_n}(s)$. Explicitly, we define $x^{(l)}_{\text{LACO},n}$ and a periodic signal $s^{(l)}_n$ with period $N/2^L$ as

$$\begin{aligned} x^{(l)}_{\text{LACO},n} &= \sum_{i=1}^{l} \left\lfloor x^{(i)}_{\text{A},n} \right\rfloor_c, \; n = 0, 1, \ldots, N-1, \\ s^{(l)}_n &= \max_{0 \le k \le 2^l - 1} \left\{ x^{(l)}_{\text{LACO},n+kN/2^l} \right\}, \end{aligned} \tag{15}$$

where $x^{(l)}_{\text{LACO},n}$ represents the superimposed signal of the first l layers, and $s^{(l)}_n$ denotes the maximum value of the sequence $\left\{x^{(l)}_{\text{LACO},n+kN/2^l}, 0 \le k \le 2^l - 1\right\}$. In this case, we have $s_n = s^{(l)}_n$ when L layers are adopted in the dimmable RLACO-OFDM.

According to the Central Limit Theorem, the time-domain OFDM signal $x_{A,n}^{(l)}$ approximates a Gaussian distribution for a large N, e.g., $N \geq 64$. We express the clipped ACO-OFDM of the l-th layer as $x_{c,n}^{(l)} = \left\lfloor x_{A,n}^{(l)} \right\rfloor_c$. From [29], the joint PDF of the ACO-OFDM signal pair $\left(x_{c,n}^{(l)}, x_{c,n+N/2^l}^{(l)}\right)$ in the l-th layer follows

$$f_{x_{c,n}^{(l)}, x_{c,n+\frac{N}{2^l}}^{(l)}}(x_1, x_2) = \frac{u(x_1)}{\sqrt{2\pi}\sigma_l} e^{-\frac{x_1^2}{2\sigma_l^2}} \delta(x_2) + \frac{u(x_2)}{\sqrt{2\pi}\sigma_l} e^{-\frac{x_2^2}{2\sigma_l^2}} \delta(x_1), \tag{16}$$

where $\delta(\cdot)$ is the Dirac delta function, $u(\cdot)$ is the Heaviside step function, and $\sigma_l = \sigma/\sqrt{2^l}$ denotes the variance of the unclipped signal $x_{A,n}^{(l)}$ [20]. Furthermore, since we have

$$s_n^{(1)} = \max\left\{x_{\text{LACO},n}^{(1)}, x_{\text{LACO},n+N/2}^{(1)}\right\} = \max\left\{x_{c,n}^{(1)}, x_{c,n+N/2}^{(1)}\right\}, \tag{17}$$

the cumulative distribution function (CDF) of $s_n^{(1)}$ is calculated as

$$\begin{aligned} F_1(s) &= P(s_n^{(1)} < s) = P\left(x_{c,n}^{(1)} < s, x_{c,n+\frac{N}{2}}^{(1)} < s\right) \\ &= \int_0^s \frac{u(x_1)}{\sqrt{2\pi}\sigma_1} e^{-\frac{x_1^2}{2\sigma_1^2}} dx_1 + \int_0^s \frac{u(x_2)}{\sqrt{2\pi}\sigma_1} e^{-\frac{x_2^2}{2\sigma_1^2}} dx_2, \end{aligned} \tag{18}$$

where $P(A)$ denotes the probability of event A. Therefore, we have PDF of $s_n^{(1)}$ as

$$f_1(s) = \frac{dF_1(s)}{ds} = \frac{2u(s)}{\sqrt{2\pi}\sigma_1} e^{-s^2/2\sigma_1^2}. \tag{19}$$

Furthermore, in Appendix A, we derive the relationship between the PDFs of $s_n^{(l)}$ and $s_n^{(l-1)}$, which is expressed as

$$\begin{aligned} f_l(s) = {} & 2\int_0^s f_{l-1}(s - x_1) \frac{1}{\sqrt{2\pi}\sigma_l} e^{-\frac{x_1^2}{2\sigma_l^2}} dx_1 \int_0^s f_{l-1}(z_2) dz_2 \\ & + 2f_{l-1}(s) \int_0^s \int_0^{z_1} f_{l-1}(z_1 - x_1) \frac{1}{\sqrt{2\pi}\sigma_l} e^{-\frac{x_1^2}{2\sigma_l^2}} dx_1 dz_1. \end{aligned} \tag{20}$$

Now, it is readily to compute the PDF of $s_n^{(l)}$ numerically by the following recursive procedure:

1) Initialization: The PDF of $s_n^{(1)}$ in (19).
2) Calculation: While $l \leq L$, evaluate $f_l(s)$ using $f_{l-1}(s)$ based on (20).

Note that closed-form expressions of $f_l(s)$ for $l \geq 2$ is difficult to achieve. Based on the definition of definite integral, we resort to the numerical calculation of $f_L(s)$ through the above procedure. Since we have $s_n = s_n^{(l)}$, the PDF of s_n is given by $f_{s_n}(s) = f_L(s)$. To show the accuracy of our analysis, both analytical and simulation results are presented in Fig. 3. One can observe that the analytical curves well match the numerical results, indicating the validity and preciseness of the above analysis.

Based on the calculated PDF, expectations of $x_{\text{LACO},n}$ and s_n can be readily obtained. Afterwards, the dimming level achieved by the proposed scheme is characterized by substituting (13) into (11) as

$$\gamma = \begin{cases} \frac{(I_H - I_L - a_2)\rho + a_1}{I_H - I_L}, & \gamma \leq 0.5, \\ 1 - \frac{(I_H - I_L - a_2)\rho + a_1}{I_H - I_L}, & \gamma > 0.5. \end{cases} \tag{21}$$

From (21), we observe that the dimming level supported by the proposed scheme varies linearly with the duty cycle for both $\gamma > 0.5$ and $\gamma \leq 0.5$. A relatively higher dimming level can be achieved when enlarging the duty cycle for $\gamma \leq 0.5$. Then, the dimming level can be further increased for $\gamma > 0.5$ by decreasing the duty cycle. Therefore, the proposed scheme has the ability of providing various dimming levels by adjusting the duty cycle of the PWM signal. Additionally, given a target dimming

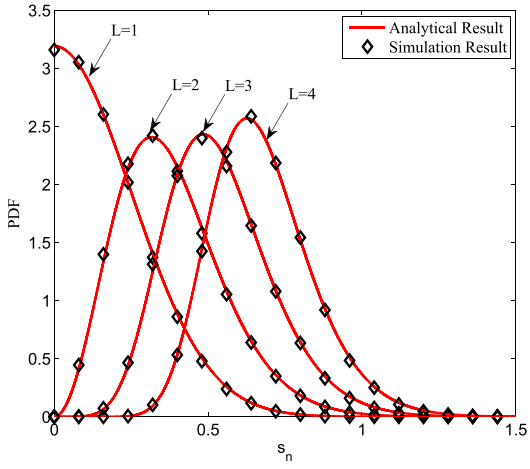

Fig. 3. Analytical and simulation results for the PDF of the signal s_n.

TABLE 1
Parameters of the Dimmable VLC System

Parameter	Value
FFT size	$N = 256$
Number of layers	L =4
BER target	2×10^{-3}
Minimum allowed current	$I_L = 1$
Maximum allowed current	$I_H = 1$

level, the desired duty cycle to satisfy the illumination requirement can be readily calculated based on (21).

5. Simulation Results and Discussion

Simulation results are presented in this section to evaluate the performance of the proposed dimming scheme. The key simulation parameters of the dimmable VLC system are summarized in Table 1. To estimate the clipping distortion of the LACO-OFDM signal, we define the scaling factor as $\beta = (I_H - I_L)/\sigma$. When the scaling factor is large enough, the probability of clipped signal would be very small and the clipping distortion can be suppressed. For example, the probability of the clipped signal would be less than 0.003 when the scaling factor satisfies $\beta \geq 2.75$ [20].

Fig. 4 portrays the curves of the clipping probability of both schemes at different values of the duty cycle ρ when combined with the PWM signal for simultaneous transmission. The clipping probability is evaluated through counting the number of the signal samples in which the nonlinear clipping occurs. It is clearly observed from Fig. 4 that the clipping probability of the LACO-OFDM significantly increases upon enlarging the duty cycle of PWM. By contrast, the clipping level of RLACO-OFDM is insensitive to the duty cycle of PWM, and moreover it is noticeably lower than that of the LACO-OFDM scheme, which implies that the proposed RLACO-OFDM is capable of eliminating the nonlinear distortion in LACO-OFDM and supporting the stable performance when integrated with the PWM signal.

In Fig. 5, we provide the BER performance of the original LACO-OFDM, RLACO-OFDM and HLACO-OFDM at the different values of σ^2 with noise power of -5 dBm when using the standard LACO-OFDM receiver. The original LACO-OFDM is the one which is not integrated with the PWM signal to support the dimming control. In Fig. 5, we adopt the duty cycle of $\rho = 0.4$ for RLACO-OFDM. Similarly, the proportion of the NLACO-OFDM, denoted by α, is set to 0.4 in HLACO-OFDM.

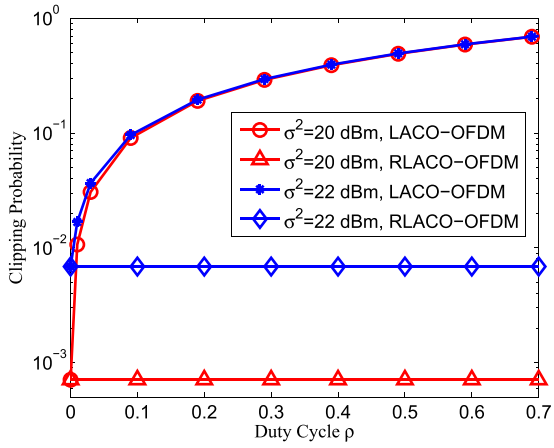

Fig. 4. Clipping probability of LACO-OFDM and RLACO-OFDM versus the duty cycle when integrated with the PWM signal.

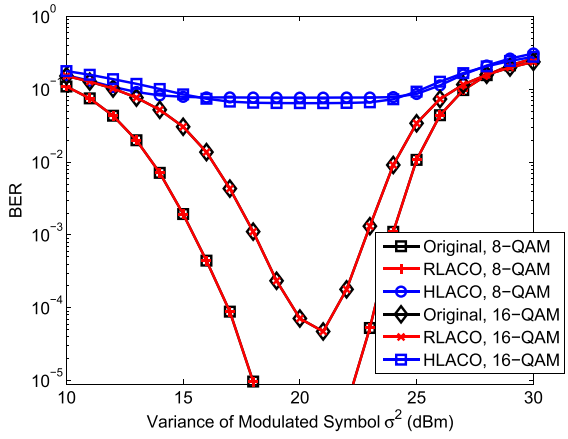

Fig. 5. BER performance of the original LACO-OFDM, the proposed RLACO-OFDM with $\rho = 0.4$ and HLACO-OFDM with $\alpha = 0.4$ at the different values of σ^2.

It is observed from Fig. 5 that the BER of RLACO-OFDM first becomes better upon the increasing of σ^2, and then deteriorates as a result of the nonlinear distortion caused by the limited dynamic range of the LED. Additionally, the RLACO-OFDM achieves the same BER performance as the original LACO-OFDM, implying that the transmitted symbols in the proposed RLACO-OFDM can be directly recovered by the conventional LACO-OFDM receiver without any performance degradation. However, HLACO-OFDM exhibits an extremely poor BER performance since no detection operation is performed before decoding to determine whether the signal belongs to LACO-OFDM or NLACO-OFDM.

Fig. 6 illustrates both analytical and simulation results of the dimming level achieved by the proposed scheme as a function of the duty cycle ρ. It can be seen in this figure that the simulation results are consistent with the theoretical analysis. Additionally, the dimming level can be linearly adjusted by varying the duty cycle ρ for $\gamma \leq 0.5$ and $\gamma > 0.5$, respectively. One can also observe that the dimming range supported by the proposed scheme is stretched as the scaling factor β increases. Therefore, the relatively low or high desired dimming levels can be achieved by utilizing a larger scaling factor β, at the cost of a low effective power of the RLACO-OFDM transmission.

The achievable spectral efficiency of the RLACO-OFDM is presented in Fig. 7 and Fig. 8 under different noise power scenarios, in which the performance of the conventional digital dimming schemes, including hybrid LACO-OFDM (HLACO-OFDM) [27], HACO-OFDM based scheme [21],

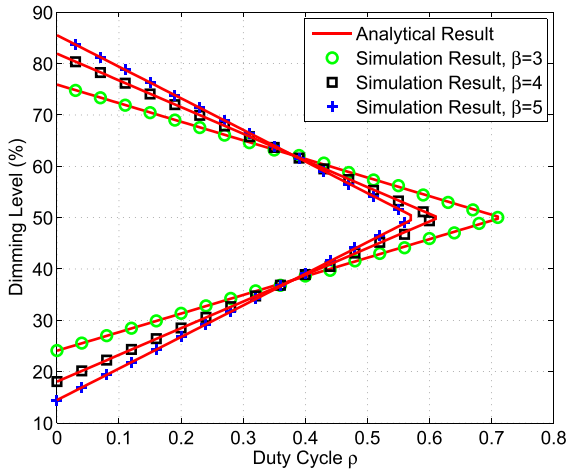

Fig. 6. Dimming level as a function of the duty cycle ρ.

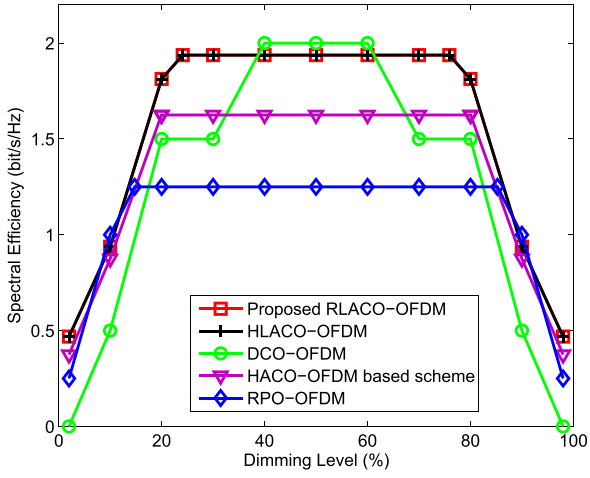

Fig. 7. Achievable spectral efficiency of different dimmable O-OFDM schemes with the noise power of −3 dBm.

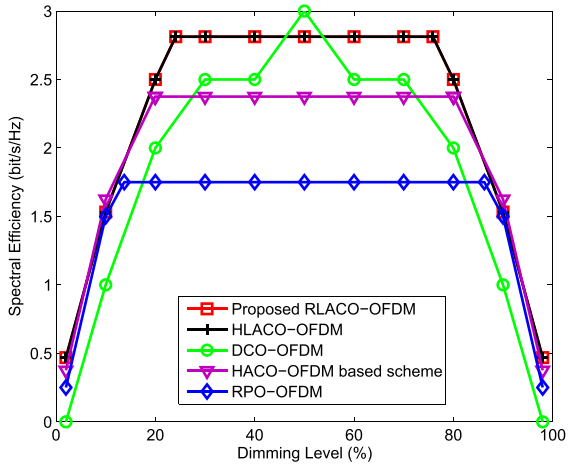

Fig. 8. Achievable spectral efficiency of different dimmable O-OFDM schemes with the noise power of −8 dBm.

and RPO-OFDM [24], are also provided for comparison. In order to provide a more comprehensive evaluation, we consider the noise power of -3 dBm and -8 dBm [24], which correspond to the scenarios of the relatively high and low noise, respectively. In the dimming range of 25%$\sim$75%, the scaling factor of the proposed scheme is set to $\beta = 3$. The scaling factor β is further enlarged to achieve the corresponding lower or higher dimming levels. By observing Figs. 7 and 8, we find that the RLACO-OFDM supports higher achievable spectral efficiency than the other dimmable O-OFDM schemes in a broad range of dimming levels. Furthermore, the proposed RLACO-OFDM achieves the same performance as the HLACO-OFDM in terms of the achievable spectral efficiency. However, additional detection operation to distinguish the transmitted LACO-OFDM and NLACO-OFDM signals is required in HLACO-OFDM before decoding [27]. Superior to the HLACO-OFDM, the decoding process of the RLACO-OFDM can be directly accomplished by the conventional LACO-OFDM receiver. This superiority will be even more pronounced especially in multiple-LED scenarios when the transmitted dimming signals are coupled and difficult to de-multiplex.

6. Conclusion

In this paper, a dimming compatible RLACO-OFDM scheme incorporating the PWM technique is conceived for VLC to provide the functionalities of both dimming control and broadband communication. Insensitive to the dimming requirements of the LEDs, the decoding process of the transmitted symbols in the proposed scheme can be readily completed by the standard LACO-OFDM receiver architecture, while no additional detection operation of the PWM dimming signal is required. Simulations have verified that the dimming level can be linearly adjusted by varying the duty cycle of the PWM signal for $\gamma \leq 0.5$ and $\gamma > 0.5$, respectively. Moreover, the proposed dimming scheme is capable of supporting a relatively stable and high achievable spectral efficiency in a wide range of dimming levels.

In the context of VLC, amalgamating the techniques of multiple-input multiple-output (MIMO) and O-OFDM is deemed as an effective way to achieve high data rate and improve communication reliability. In order to support the dual functionalities of high-speed communication and indoor illumination in VLC, we intend to integrate the proposed RLACO-OFDM with MIMO and explore the potential transmission capacity of the dimmable MIMO VLC system in future work.

Appendix
Detailed derivation of (20)

Based on the definition in (15), $s_n^{(l)}$ is the maximum value in the sequence $\{x^{(l)}_{\mathrm{LACO},n+kN/2^l}, 0 \leq k \leq 2^l - 1\}$. We can express k as

$$k = \begin{cases} 2k', & k \text{ is even}, \\ 2k' + 1, & k \text{ is odd}, \end{cases} \tag{22}$$

where $0 \leq k' \leq 2^{l-1} - 1$. Then, $x^{(l)}_{\mathrm{LACO},n+kN/2^l}$ can be rewritten as

$$x^{(l)}_{\mathrm{LACO},n+kN/2^l} = \begin{cases} x^{(l)}_{\mathrm{LACO},n+\frac{k'N}{2^{l-1}}}, & k \text{ is even}, \\ x^{(l)}_{\mathrm{LACO},n+\frac{N}{2^l}+\frac{k'N}{2^{l-1}}}, & k \text{ is odd}. \end{cases} \tag{23}$$

Then defining

$$\begin{aligned} z_n^{(l)} &\triangleq \max_{0 \leq k' \leq 2^{l-1}-1} \left\{ x^{(l)}_{\mathrm{LACO},n+\frac{k'N}{2^{l-1}}} \right\}, \\ z_{n+N/2^l}^{(l)} &\triangleq \max_{0 \leq k' \leq 2^{l-1}-1} \left\{ x^{(l)}_{\mathrm{LACO},n+\frac{N}{2^l}+\frac{k'N}{2^{l-1}}} \right\}, \end{aligned} \tag{24}$$

we can write

$$s_n^{(l)} = \max\left\{z_n^{(l)}, z_{n+N/2^l}^{(l)}\right\}. \tag{25}$$

Now observing $z_n^{(l)}$, it gives

$$\begin{aligned} z_n^{(l)} &= \max_{0\le k'\le 2^{l-1}-1}\left\{x_{\mathrm{LACO},n+\frac{k'N}{2^{l-1}}}^{(l-1)} + x_{\mathrm{A},n+\frac{k'N}{2^{l-1}}}^{(l)}\right\} \\ &= \max_{0\le k'\le 2^{l-1}-1}\left\{x_{\mathrm{LACO},n+\frac{k'N}{2^{l-1}}}^{(l-1)}\right\} + x_{\mathrm{A},n}^{(l)} \\ &= s_n^{(l-1)} + x_{\mathrm{A},n}^{(l)}, \end{aligned} \tag{26}$$

where we use the fact that $x_{\mathrm{A},n}^{(l)} = x_{\mathrm{A},n+k'N/2^{l-1}}^{(l)}$ since $x_{\mathrm{A},n}^{(l)}$ is a periodic signal with period of $N/2^{l-1}$. Similarly, we have

$$z_{n+N/2^l}^{(l)} = s_{n+N/2^l}^{(l-1)} + x_{\mathrm{A},n+N/2^l}^{(l)}. \tag{27}$$

Then, the joint PDF of $z_n^{(l)}$ and $z_{n+N/2^l}^{(l)}$ can be calculated as

$$f_{z_n^{(l)}, z_{n+\frac{N}{2^l}}^{(l)}}(z_1, z_2) = \int_{-\infty}^{+\infty}\int_{-\infty}^{+\infty} f_{s_n^{(l-1)}, s_{n+\frac{N}{2^l}}^{(l-1)}}(z_1 - x_1, z_2 - x_2)\, f_{x_{\mathrm{A},n}^{(l)}, x_{\mathrm{A},n+\frac{N}{2^l}}^{(l)}}(x_1, x_2)\, dx_1 dx_2. \tag{28}$$

Here, $f_{s_n^{(l-1)}, s_{n+N/2^l}^{(l-1)}}(s_1, s_2)$ denotes the joint PDF of $s_n^{(l-1)}$ and $s_{n+N/2^l}^{(l-1)}$, and $f_{x_{\mathrm{A},n}^{(l)}, x_{\mathrm{A},n+N/2^l}^{(l)}}(x_1, x_2)$ is the joint PDF of $x_{\mathrm{A},n}^{(l)}$ and $x_{\mathrm{A},n+N/2^l}^{(l)}$ which is given in (16). Note that $s_n^{(l)}$ and $s_{n+N/2^l}^{(l)}$ are independent and they obey the same probability distribution. Hence, $f_{s_n^{(l)}, s_{n+N/2^l}^{(l)}}(s_1, s_2)$ can be expressed as

$$f_{s_n^{(l-1)}, s_{n+N/2^l}^{(l-1)}}(s_1, s_2) = f_{l-1}(s_1) f_{l-1}(s_2). \tag{29}$$

Additionally, since $s_n^{(l-1)}$ and $s_{n+N/2^l}^{(l-1)}$ are nonnegative signals, we have $f_{l-1}(s_1) = 0$ and $f_{l-1}(s_2) = 0$ for $s_1 < 0$ and $s_2 < 0$, respectively. Then, we arrive at the expression of $f_{z_n^{(l)}, z_{n+N/2^l}^{(l)}}(z_1, z_2)$ by using (29) in (28), which is given by

$$\begin{aligned} f_{z_n^{(l)}, z_{n+N/2^l}^{(l)}}(z_1, z_2) = &\int_{-\infty}^{\infty}\int_{-\infty}^{\infty} f_{l-1}(z_1 - x_1)\, f_{l-1}(z_2 - x_2) \\ &* \left[\frac{u(x_1)}{\sqrt{2\pi}\sigma_l} e^{-\frac{x_1^2}{2\sigma_l^2}} \delta(x_2) + \frac{u(x_2)}{\sqrt{2\pi}\sigma_l} e^{-\frac{x_2^2}{2\sigma_l^2}} \delta(x_1)\right] dx_1 dx_2 \\ = &\int_0^{z_1} f_{l-1}(z_1 - x_1)\, f_{l-1}(z_2)\, \frac{1}{\sqrt{2\pi}\sigma_l} e^{-\frac{x_1^2}{2\sigma_l^2}} dx_1 \\ &+ \int_0^{z_2} f_{l-1}(z_2 - x_2)\, f_{l-1}(z_1)\, \frac{1}{\sqrt{2\pi}\sigma_l} e^{-\frac{x_2^2}{2\sigma_l^2}} dx_2. \end{aligned} \tag{30}$$

The CDF of $s_n^{(l)}$ is calculated as

$$F_l(s) = P\left(z_n^{(l)} \le s, z_{n+N/2^l}^{(l)} \le s\right) = \int_0^s \int_0^s f_{z_n^{(l)}, z_{n+N/2^l}^{(l)}}(z_1, z_2)\, dz_1 dz_2. \tag{31}$$

Using (31) and taking the derivative of $F_l(s)$ with respect to s, we obtain the relationship between the PDFs of $s_n^{(l)}$ and $s_n^{(l-1)}$, as desired in (20).

References

[1] D. Karunatilaka, F. Zafar, V. Kalavally, and R. Parthiban, "LED based indoor visible light communications: State of the art," *IEEE Commun. Surveys Tut.*, vol. 17, no. 3, pp. 1649–1678, Mar. 2015.

[2] H. Haas, L. Yin, Y. Wang, and C. Chen, "What is LiFi?" *J. Lightw. Technol.*, vol. 34, no. 6, pp. 1533–1544, Mar. 2016.

[3] Y. Wang, N. Chi, Y. Wang, L. Tao, and J. Shi, "Network architecture of a high-speed visible light communication local area network," *IEEE Photon. Technol. Lett.*, vol. 27, no. 2, pp. 197–200, Jan. 2015.

[4] S. Buzzi, C.-L. I, T. E. Klein, H. V. Poor, C. Yang, and A. Zappone, "A survey of energy-efficient techniques for 5G networks and challenges ahead," *IEEE J. Sel. Areas Commun.*, vol. 34, no. 4, pp. 697–709, Apr. 2016.

[5] M. Ayyash *et al.*, "Coexistence of WiFi and LiFi toward 5G: Concepts, opportunities, and challenges," *IEEE Commun. Mag.*, vol. 54, no. 2, pp. 64–71, Feb. 2016.

[6] X. Huang *et al.*, "2.0-Gb/s visible light link based on adaptive bit allocation OFDM of a single phosphorescent white LED," *IEEE Photon. J.*, vol. 7, no. 5, Oct. 2015, Art. no. 7904008.

[7] I. Lu, C. Yeh, D. Hsu, and C. Chow, "Utilization of 1-GHz VCSEL for 11.1-Gbps OFDM VLC wireless communication," *IEEE Photon. J.*, vol. 8, no. 3, Jun. 2016, Art. no. 7904106.

[8] K.-T. Ho *et al.*, "3.2 Gigabit-per-second visible light communication link with InGaN/GaN MQW micro-photodetector," *Opt. Exp.*, vol. 26, no. 3, pp. 3037–3045, Feb. 2018.

[9] J. Armstrong, "OFDM for optical communications," *J. Lightw. Technol.*, vol. 27, no. 3, pp. 189–204, Feb. 2009.

[10] J. B. Carruthers and J. M. Kahn, "Multiple-subcarrier modulation for nondirected wireless infrared communication," *IEEE J. Sel. Areas Commun.*, vol. 14, no. 3, pp. 538–546, Apr. 1996.

[11] S. D. Dissanayake and J. Armstrong, "Comparison of ACO-OFDM, DCO-OFDM and ADO-OFDM in IM/DD systems," *J. Lightw. Technol.*, vol. 31, no. 7, pp. 1063–1072, Apr. 2013.

[12] J. Armstrong and A. J. Lowery, "Power efficient optical OFDM," *Electron. Lett.*, vol. 42, no. 6, pp. 370–372, Mar. 2006.

[13] S. C. J. Lee, S. Randel, F. Breyer, and A. M. J. Koonen, "PAM-DMT for intensity-modulated and direct-detection optical communication systems," *IEEE Photon. J.*, vol. 21, no. 23, pp. 1749–1751, Dec. 2009.

[14] B. Ranjha and M. Kavehrad, "Hybrid asymmetrically clipped OFDM-based IM/DD optical wireless system," *IEEE/OSA J. Opt. Commun. Netw.*, vol. 6, no. 4, pp. 387–396, Apr. 2014.

[15] Q. Wang, C. Qian, X. Guo, Z. Wang, D. G. Cunningham, and I. H. White, "Layered ACO-OFDM for intensity-modulated direct-detection optical wireless transmission," *Opt. Exp.*, vol. 23, no. 9, pp. 12382–12393, May 2015.

[16] J. Gancarz, H. Elgala, and T. D. C. Little, "Impact of lighting requirements on VLC systems," *IEEE Commun. Mag.*, vol. 51, no. 12, pp. 34–41, Dec. 2013.

[17] F. Zafar, D. Karunatilaka, and R. Parthiban, "Dimming schemes for visible light communication: The state of research," *IEEE Wireless Commun.*, vol. 22, no. 2, pp. 29–35, Apr. 2015.

[18] Q. Wang, Z. Wang, and L. Dai, "Asymmetrical hybrid optical OFDM for visible light communications with dimming control," *IEEE Photon. Technol. Lett.*, vol. 27, no. 9, pp. 974–977, May 2015.

[19] Y. Yang, Z. Zeng, J. Cheng, and C. Guo, "An enhanced DCO-OFDM scheme for dimming control in visible light communication systems," *IEEE Photon. J.*, vol. 8, no. 3, Jun. 2016, Art. no. 7904813.

[20] Q. Wang, Z. Wang, L. Dai, and J. Quan, "Dimmable visible light communications based on multilayer ACO-OFDM," *IEEE Photon. J.*, vol. 8, no. 3, Jun. 2016, Art. no. 7905011.

[21] F. Yang and J. Gao, "Dimming control scheme with high power and spectrum efficiency for visible light communications," *IEEE Photon. J.*, vol. 9, no. 1, Feb. 2017, Art. no. 7901612.

[22] Z. Wang, W.-D. Zhong, C. Yu, J. Chen, C. P. S. Francois, and W. Chen, "Performance of dimming control scheme in visible light communication system," *Opt. Exp.*, vol. 20, no. 17, pp. 18861–18868, Aug. 2012.

[23] G. Ntogari, T. Kamalakis, J. Walewski, and T. Sphicopoulos, "Combining illumination dimming based on pulse-width modulation with visible-light communications based on discrete multitone," *IEEE/OSA J. Opt. Commun. Netw.*, vol. 3, no. 1, pp. 56–65, Jan. 2011.

[24] H. Elgala and T. D. C. Little, "Reverse polarity optical-OFDM (RPO-OFDM): Dimming compatible OFDM for gigabit VLC links," *Opt. Exp.*, vol. 21, no. 20, pp. 24288–24299, Oct. 2013.

[25] Q. Wang, Z. Wang, and L. Dai, "Multiuser MIMO-OFDM for visible light communications," *IEEE Photon. J.*, vol. 7, no. 6, Dec. 2015, Art. no. 7904911.

[26] Y. Tao, X. Liang, J. Wang, and C. Zhao, "Scheduling for indoor visible light communication based on graph theory," *Opt. Exp.*, vol. 23, no. 3, pp. 2737–2752, Feb. 2015.

[27] Y. Sun, F. Yang, and J. Gao, "Novel dimmable visible light communication scheme based on hybrid LACO-OFDM," *J. Lightw. Technol.*, vol. 36, no. 20, pp. 4942–4951, Oct. 2018.

[28] X. Zhang, Q. Wang, R. Zhang, S. Chen, and L. Hanzo, "Performance analysis of layered ACO-OFDM," *IEEE Access*, vol. 5, pp. 18366–18381, 2017.

[29] W. Xu, M. Wu, H. Zhang, X. You, and C. Zhao, "ACO-OFDM-specified recoverable upper clipping with efficient detection for optical wireless communications," *IEEE Photon. J.*, vol. 6, no. 5, Oct. 2014, Art. no. 7902617.